Far-field of GaN film-transferred green light-emitting diodes with two-dimensional photonic crystals

Chun-Feng Lai[1], Jim-Yong Chi[2*], Hao-Chung Kuo[1*], Hsi-Hsuan Yen[1], Chia-En Lee[1], Chia-Hsin Chao[3], Han-Tsung Hsueh[3] and Wen-Yung Yeh[3]

[1] *Department of Photonics and Institute of Electro-Optical Engineering, National Chiao-Tung University, Hsinchu 300, Taiwan, R.O.C.*

[2] *Institute of Optoelectronic Engineering, National Dong-Hua University, Hualien 97401, Taiwan, R.O.C.*

[3] *Electronics and Opto-electronics Research Laboratories, Industrial Technology Research Institute, Hsinchu 310, Taiwan, R.O.C.*

[*] *Corresponding author: chij@mail.ndhu.edu.tw, hckuo@faculty.nctu.edu.tw*

Abstract: Far-field distributions of GaN-based photonic crystal (PhC) film-transferred light-emitting diodes (FT-LEDs) were investigated. The thickness of the device is about 840 nm. The emission wavelength is around 520 nm. The PhC region is a square lattice with a/λ around 0.5. Angular-resolved measurements in the Γ-*X* and Γ-*M* directions were made in the polarized-resolved manner. Guided mode extraction behavior in agreement with the two-dimensional free-photon band calculation was observed. In addition, the pseudo-TM behavior for the non-collinearly coupled modes was observed. The azimuthal-mapping of the angular-resolved spectra revealed the evolution of the collinearly and the non-collinearly coupled modes. Furthermore, the light enhancement of ~2.7x and the collimation angle about 102.3° were achieved.

OCIS codes: (230.3670) Light-emitting diodes; (230.5298) Photonic crystals.

References and links

1. M. R. Krames, O. B. Shchekin, R. Mueller-Mach, G. O. Mueller, L. Zhou, G. Harbers, and M. G. Craford, "Status and Future of High-Power Light-Emitting Diodes for Solid-State Lighting" J. Disp. Technol., **3**, 160-175 (2007).
2. A. David, C. Meier, R. Sharma, F. S. Diana, S. P. DenBaars, E. Hu, S. Nakamura, and C. Weisbuch, "Photonic bands in two-dimensionally patterned multimode GaN waveguides for light extraction" Appl. Phys. Lett., **87**, 101107-1-101107-3 (2005).
3. C. F. Lai, J. Y. Chi, H. C. Kuo, C. H. Chao, H. T. Hsueh, J. –F. T. Wang, and W. Y. Yeh, "Anisotropy of light extraction from GaN two-dimensional photonic crystal light-emitting diodes," Opt. Express **16**, 7285-7294 (2008).
4. J. J. Wierer, M. R. Krames, J. E. Epler, N. F. Gardner, and M. G. Craford, "InGaN/GaN quantum-well heterostructure light-emitting diodes employing photonic crystal structures, " Appl. Phys. Lett. **84**, 3885-3887 (2004).
5. K. McGroddy, A. David, E. Matioli, M. Iza, S. Nakamura, S. DenBaars, J. S. Speck, C. Weisbuch, and E. L. Hu, "Directional emission control and increased light extraction in GaN photonic crystal light emitting diodes," Appl. Phys. Lett., **93**, 103502-1-103502-3 (2008).
6. C. F. Lai, J. Y. Chi, H. H. Yen, H. C. Kuo, C. H. Chao, H. T. Hsueh, J.-F. T. Wang, C. Y. Huang, and W. Y. Yeh, "Polarized light emission from photonic crystal light-emitting diodes," Appl. Phys. Lett. **92**, 243118-1-243118-3 (2008).
7. A. David, T. Fujii, B. Moran, S. Nakamura, S. P. DenBaars, and C. Weisbuch, "Photonic crystal laser lift-off GaN light-emitting diodes," Appl. Phys. Lett., **88**, 133514-1-133514-3 (2006).
8. H. K. Cho, S. K. Kim, D. K. Bae, B. C. Kang, J. S. Lee, and Y. H. Lee, "Laser Liftoff GaN Thin-Film Photonic Crystal GaN-Based Light-Emitting Diodes," IEEE Photon. Technol. Lett., **20**, 2096-2098 (2008).
9. C. F. Lai, C. H. Chao, H. C. Kuo, C. E. Lee, and W. Y. Yeh, "Directional light extraction enhancement from GaN-based film-transferred photonic crystal light-emitting diodes," Appl. Phys. Lett. **94**, 123106-1-123106-3 (2009).
10. Bergenek, Ch. Wiesmann, H. Zull, R. Wirth, P. Sundgren, N. Linder, K. Streubel, and T. F. Krauss, "Directional light extraction from thin-film resonant cavity light-emitting diodes with a photonic crystal," Appl. Phys. Lett. **93**, 231109-1-231109-3 (2008).

#107988 - $15.00 USD Received 2 Mar 2009; revised 4 May 2009; accepted 5 May 2009; published 11 May 2009

11. C. E. Lee, C. F. Lai, Y. C. Lee, H. C. Kuo, T. C. Lu, and S. C. Wang, "Nitride-Based Thin-Film Light-Emitting Diodes With Photonic Quasi-Crystal Surface," IEEE Photon. Technol. Lett., **21**, 331-333 (2009).
12. F. S. Diana, A. David, I. Meinel, R. Sharma, C. Weisbuch, S. Nakamura, and P. M. Petroff, "Photonic Crystal-Assisted Light Extraction from a Colloidal Quantum Dot/GaN Hybrid Structure," Nano Lett. **6**, 1116-1120 (2006).
13. M. F. Schubert, S. Chhajed, J. K. Kim, E. F. Schubert, and J. Cho, "Polarization of light emission by 460 nm GaInN/GaN light-emitting diodes grown on (0001) oriented sapphire substrates," Appl. Phys. Lett. **91**, 051117-1-051117-3 (2007).
14. J. J. Wierer, A. David, and M. M. Megens, Nature Photonics, **3**, 163-169 (2009).
15. S. Schad, B. Neubert, C. Eicher, M. Scherer, F. Habel, M, Seyboth, F. Scholz, D. Hofstetter, P. Unger, W. Schmid, S. Karnutsch, and K. Streubel, "Absorption and light scattering in InGaN-on-sapphire- and AlGaInP-based light-emitting diodes," IEEE J. Lightwave Technol. **22**, 2323-2332 (2004).
16. A. David, T. Fujii, E. Matioli, R. Sharma, S. Nakamura, S. P. DenBaars, and C. Weisbuch, "GaN light-emitting diodes with Archimedean lattice photonic crystals," Appl. Phys. Lett., **88**, 073510-1-073510-3 (2006).
17. T. Ochiai, and K. Sakoda, "Nearly free-photon approximation for two-dimensional photonic crystal slabs," Phys. Rev. B **64**, 045108-1-045108-11, (2001).
18. M. Imada, A. Chutinan, S. Noda, and M. Mochizuki, "Multidirectionally distributed feedback photonic crystal lasers," Phys. Rev. B, **65**, 195306-1-195306-3 (2002).
19. A. David, H. Benisty, and C. Weisbuch, "Spontaneous emission in GaN/InGaN photonic crystal nanopillars," Opt. Express **15**, 17991-18004 (2007).

1. Introduction

To switch on light-emitting diode (LED) applications in the next-generation projector displays and automobile headlights, further improvements of the light extraction efficiency and the emission patterns are required [1]. Approaches based on the photonic crystal (PhC) have attracted attention for improved light extraction from GaN LEDs [2-3] and for controlling the collimating and polarization properties of the extracted lights [4-6]. However, a large portion of the generated light can still be trapped within the GaN and sapphire layers in the form of guided modes due to the total internal reflection (TIR). Thus, the approach to reduce the number of guided modes in the waveguide by reducing the LED thickness is of interest such as FT-LEDs. The GaN-based FT-LED combined with PhC has been reported for the *blue* wavelength range [7-9]. Recently, an AlInGaP thin-film LED combined with PhC and a distributed Bragg reflector (DBR) reflector was reported for enhancing light extraction efficiency and temperature stability in the *red* wavelength range [10]. In the present work, a GaN-based PhC FT-LEDs emitting the *green* (λ = 520 nm) color has been fabricated and studied. Angular-resolved electroluminescence (EL) spectra was measured in the polarized-resolved manner and compared with the band structure calculation. The far-field angular distribution for different wavelength has also been mapped by rotating the sample to reveal the guided modes evolution in the azimuthal plane. The polarization properties of these green FT-LEDs are also examined since the light extracted with the PhC is generally polarized. Such a polarization property may make the PhC extracted light source to have different reflection properties from the conventional illumination sources.

2. Experimental

The green GaN LED wafers were grown by metal organic chemical vapor deposition (MOCVD) onto c-face (0001) 2 in. diameter sapphire substrates. The LED structure consists of a 30-nm-thick GaN nucleation layer, a 4-μm-thick un-doped GaN buffer layer, a 3-μm-thick Si-doped n-GaN layer, a 180 nm InGaN/GaN multiple quantum well (MQW) active region with 10 periods of 3/15 nm well/ barrier width (dominant wavelength λ = 520 nm), a 20-nm-thick Mg-doped p-AlGaN electron blocking layer, a 370 nm thick Mg-doped p-GaN contact layer. After growth, that epitaxial film was transferred to Si wafer carrier and the sapphire substrate was removed with the laser lift-off technique. The wafer processing of GaN FT-LEDs associated PhC was the same as in Ref. 11. The resulting structure was then thinned down by chemical-mechanical polishing (CMP) to obtain the

#107988 - $15.00 USD Received 2 Mar 2009; revised 4 May 2009; accepted 5 May 2009; published 11 May 2009

"4λ" effective cavity with thickness ~840 nm. Then the residue was removed with an oxygen reactive ion etch (RIE); this process was found *not* to affect the current spreading over n-GaN layer. The PhC with a square lattice of circular holes was then defined by holography lithography. Holes were etched into the top n-GaN surface using inductively coupled plasma (ICP) dry etching to a depth t = 50 nm. Figure 1(a) shows the film-transferred GaN PhC LED structure cross-section of the transmission electron microscopy (TEM) image. The lattice constant, *a,* and holes diameter, *d,* of PhC are 280 and 180 nm, respectively. Inset in Fig. 1(a) depicts the square lattice PhC structure of the scanning electron microscopy (SEM) image. Finally, a patterned Ti/Al/Ti/Au (100/200/100/2000 nm) electrode was deposited on n-GaN as the n-type contact layer and Cr/Au (30/2000 nm) metal was deposited on the backside of the Si substrate. No attempt to optimize the current spreading by pad design was made for the present work. Also a thin etching depth was used due to the currently non-optimized processing condition.

After fabrication, the dies were mounted on transistor outline (TO) packages. *No* expoxy encapsulation was applied over the die. In addition, the intensity-current-voltage (*L-I-V*) characteristics were measured using an integration sphere with Si photodiode. The turn on voltage was about 2.6 V. The light output power of the GaN-based PhC FT-LED at a driving current of 350 mA shows output power enhancement by 170% (2.7x), when compared to the GaN-based FT-LED without PhC, as shown in Fig. 2(a). The external quantum efficiency (EQE) of GaN-based FT-LED with PhC and without PhC at a driving current of 350 mA was 5.57% and 2%, respectively, as shown in Fig. 2(b). The measured EQE was low due to the non-optimized chip processes and designs including pad design which may suffer current crowding at high current, chip surface treatment which may cause high series resistance, etc.. However, at low current, the light emission from the chip was uniform across the chip area as shown in Fig. 1 (b). These data are similar to that reported for the AlInGaP system except that the present work uses a metal reflector rather that a DBR structures [10].

The angular-resolved electroluminescence (EL) measurement was performed to study the far-field distribution. A motorized rotation stage was used to collect light as a function of the zenith angle with a linear analyzing polarizer, an aperture (1 mm in diameter), and an optical fiber. The collected light is dispersed by a spectrometer and analyzed by a cooled CCD detector array (1024 X 256 pixels). A continuous current of 20 mA injected into the TO mounted device at room temperature. The polarized spectra were then taken with the polarizer oriented in *s* and *p* directions. The light emission spectra were taken for every zenithal angle with 0.2 degree resolution from -90 to +90 degree. The angular-resolved were then taken by rotation in the azimuthal plane to study the evolution of the observed spectra features.

#107988 - $15.00 USD Received 2 Mar 2009; revised 4 May 2009; accepted 5 May 2009; published 11 May 2009

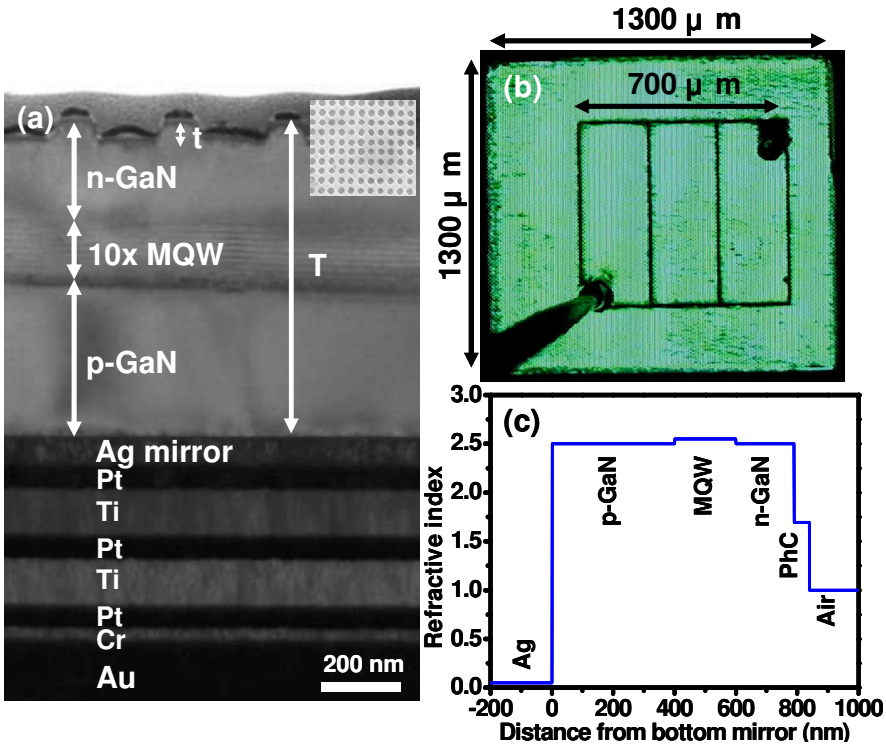

Fig. 1. (a) TEM micrograph of a GaN PhC FT-LED structure with the etch depth t = 50 nm and GaN cavity thickness T = 840 nm; the inset shown the SEM micrograph of the square lattice PhC with average value of the lattice constant a = 280 nm and the diameter of air holes d = 180 nm patterned with the holographic lithography; (b) the optical micrograph showing the green light distribution across the die operated at low injection current 5 mA ; (c) vertical effective refractive index profile of the characterized the GaN PhC FT-LED.

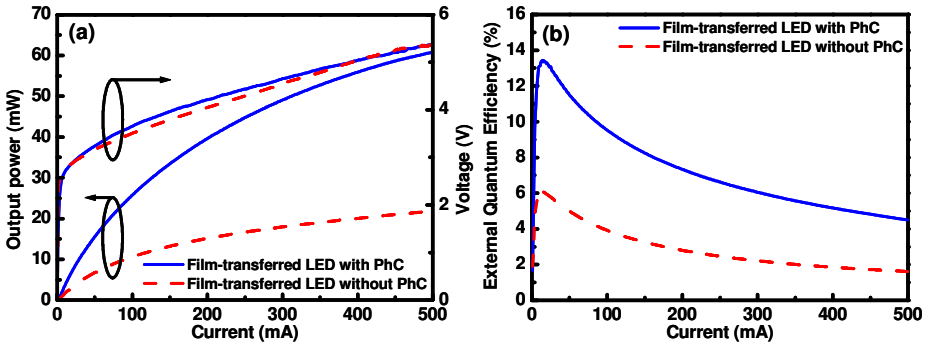

Fig. 2. (a) Light output power-current-voltage (*L-I-V*) curve and (b) external quantum efficiency characteristics of GaN–based FT-LED with PhC and without PhC.

3. Results and Discussion

The angular-resolved measurement results under electrical current injection are shown in Fig. 3. These spectra are displayed on a wavelength vs. angle plot with the color of the pixels representing the intensity of the spectra according to the color-coded scale bar shown in Fig. 3. The measured angular-resolved spectra (without polarizer) are shown in Fig. 3(a) and 3(b) with light collected along the Γ-*X* and Γ-*M* directions. The mirror symmetry of the pattern is the consequence of the isotropic nature for the light emissions with EL emission and the crystal symmetry. The sharp lines are due to the extraction of the wave guided

#107988 - $15.00 USD Received 2 Mar 2009; revised 4 May 2009; accepted 5 May 2009; published 11 May 2009

modes propagating in the GaN waveguides formed with the GaN epitaxial layers between the metal electrode at the bottom and air on top. Figure 3(a) and 3(b) also show that, for each direction of propagation, there are two families of lines with different slopes superimposed with each other. These two families of lines are identified to be the collinear or non-collinear coupling with the reciprocal vectors and are labeled as the A-type and B-type modes, respectively [2, 12]. All of these A-type and B-type modes can be accurately accounted for by the coupling of the reciprocal lattice vectors in the Γ-*M* and Γ-*X* directions with every individual mode that is confined in the slab waveguide. In order to study these modes more clearly, the spectra shown in Fig. 3(a) and 3(b) are transformed to the guided mode dispersion curves as shown in Fig. 3(c) [2]. The image shows the normalized dispersion curves for each mode lines in the Γ-*X* and Γ-*M* directions.

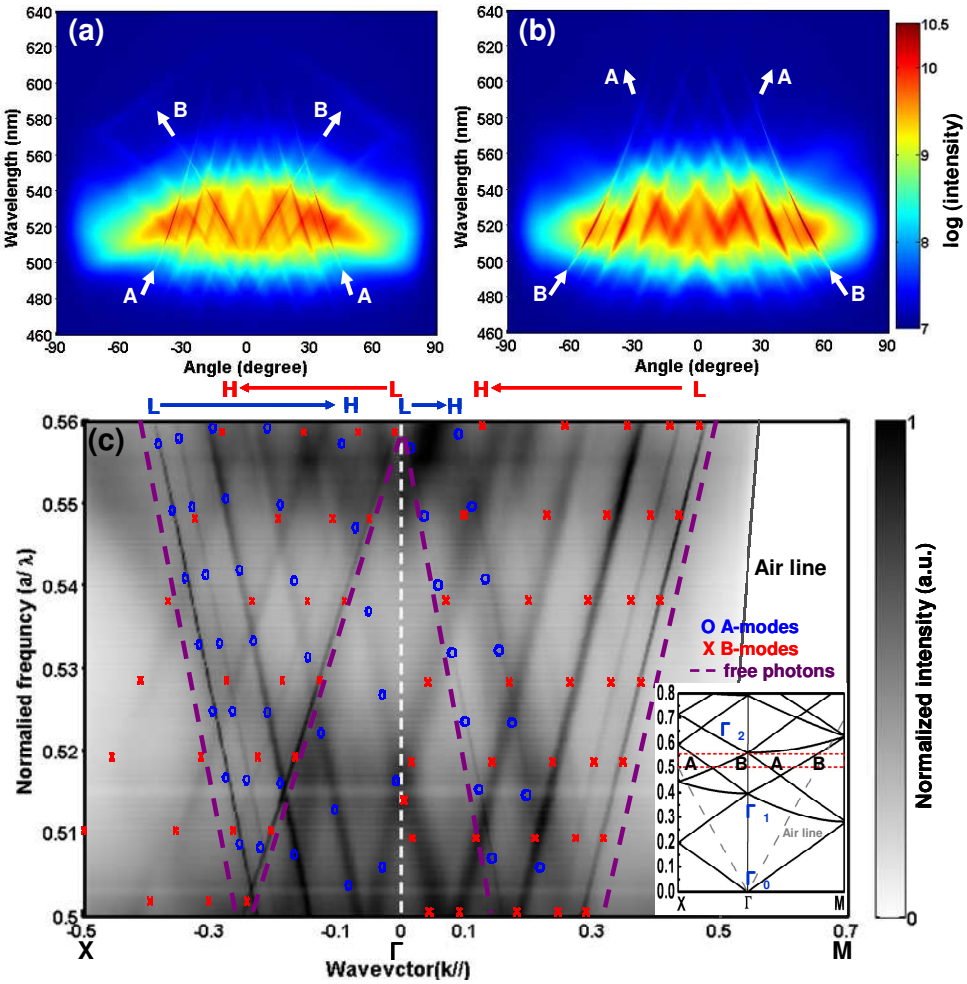

Fig. 3. Angular-resolved spectra taken along (a) Γ-*X* and (b) Γ-*M* direction without the polarizer. (c) Shows the multimode dispersion curves determined from the data shown in (a) and (b) and compared with the 2D band diagram calculated in the free photon limit with the average index $n_{GaN} = 2.52$ shown as dashed lines. The "o" and "x" marks correspond to the calculated A-type and B-type modes from the n_{eff}'s of the multimode propagating in the slab waveguide with the refractive index profile shown in Fig.1(c). Only five of the eight modes are shown. The inset in (c) is the complete free photon band structure with the region ($a/\lambda = 0.5$~0.56) studied in the present work surrounded by the box shown.

To study the observed mode lines, the guided mode distribution was calculated in a slab waveguide with the vertical effective refractive index profile show in Fig. 1(c) with the index for the metal mirror $n = 0.05+2.5i$. Since the emitted light from the MQW is predominantly TE polarized in the waveguide plane [13], only TE modes are analyzed.

#107988 - $15.00 USD Received 2 Mar 2009; revised 4 May 2009; accepted 5 May 2009; published 11 May 2009

Eight guided TE modes with effective refractive index distribution n_{eff} = [2.506, 2.436, 2.342, 2.207, 2.022, 1.769, 1.437, and 1.005] are obtained. These modes are then used to fit the observing mode lines in Fig. 3(c). The first five of the eight modes are clearly visible and can be fitted with the corresponding effective indices as blue circles and red crosses for A-type and B-type modes respectively. Good fit with the measured mode lines within experimental accuracy is evident. The two-dimensional (2D) free photon band structure with the average index $n_{GaN} = 2.52$ was also calculated and is shown in the inset of Fig. 3(c). The corresponding region for the present measurements is shown in the box. The dash lines plotted the bands in Fig. 3(c) that appeared in the boxed region of the inset. It can be seen that the measured data are in complete agreement considering the accuracy of the material constants used in the calculation. This agreement with the free photon bands indicates that the present etch depth of the holes is "shallow", consistent with the observation that "anticrossing" of the bands is absent in the present sample [7]. The rest of the high order modes become weak and less visible indicating a high absorption for the high order modes due to the possible presence of the highly absorbing interfacial layer [14-15]. Another observation is that the intensity of the mode lines with a positive slope emanating from the Γ_1 are more numerous and stronger than the negative ones emanating from Γ_2 points (see the labeling in inset of Fig. 3(c)). There are five modes that are clearly visible pointing up ward from the Γ point while there are only two in the downward direction. This happens both to the A and B modes. The reason for this behavior is most likely due to the coupling strength of the waveguide modes to reciprocal lattice vectors. The coupling strength has a cubic-dependence on the magnitude of the reciprocal lattice wave vectors [16]. Since the negatively sloped mode lines are coupled with the $G_{\Gamma M}$ while the positive ones are coupled to the $G_{\Gamma X}$ which is $1/\sqrt{2}$ that of $G_{\Gamma M}$, hence, a weaker intensity. Only three weaker intensity lines are visible in the present conditions. This behavior in intensity will be another factor to influence the far field distribution and needs to be considered in the design of the PhC LED. In addition to the angular distribution, the polarization of the output light from the film-transferred PhC LEDs is also investigated.

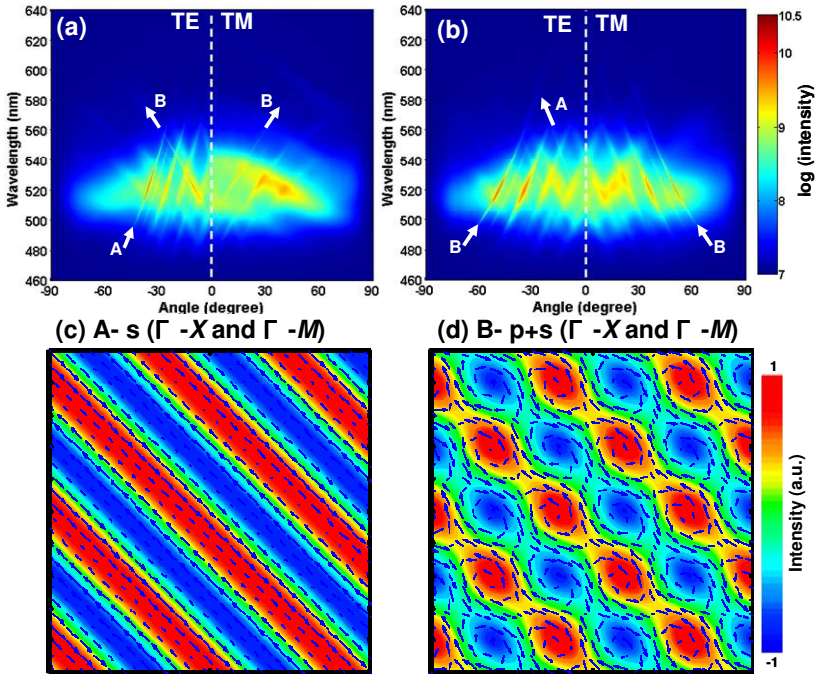

Fig. 4. The polarization angular resolved spectra taken in the (a) Γ-X and (b) Γ-M directions with the polarizer kept at the TE (left) and TM (right) orientations. Electric field distribution for (c) singly and (d) double degenerate modes at Γ point. Arrows indicate the electric field vectors in the plane.

#107988 - $15.00 USD Received 2 Mar 2009; revised 4 May 2009; accepted 5 May 2009; published 11 May 2009

In the extraction process, the PhC lattice will also influence the polarization of the emitted light. To study these effects, the polarizations of the out-coupled A-type and B-type modes are examined through a polarizer to observe the polarization of the emitted light. Figure 4 shows the angular-resolved spectra in the two directions (a) Γ-*X* and (b) Γ-*M* with the axis of the polarizer oriented parallel (TE) and perpendicular (TM) to the incident plane, respectively. It can be seen that in the Γ-*X* directions (Fig. 4(a)), the A-type modes are only visible in the TE polarization indicating a strong TE polarization with little TM components, while the B-type modes have both the TE and TM components and are visible in both the TE and TM polarization. These results indicate a larger (smaller) polarization ratio (TE/TM) for the A-type modes (B-type modes) than the B-type modes (A-type modes). Similar conclusion, but with a smaller polarization ratio [5], can be made with the modes in the Γ-*M* direction by an examination of Fig. 4(b). It is seen that the out-coupling of the B-modes is more intense than the A-modes in this direction as explained above by the coupling strength to the respective reciprocal wavevectors. Nevertheless, the A-mode is more visible in the TE orientation than in TM orientation, even though smaller TE/TM ratio is calculated for this direction [6]. While for the B-modes, the mode lines appeared in both the TE and TM polarization as shown in Fig. 4(b). This property of the B-type mode lines is consistent with the pseudo-TM nature of the B-modes. Due to the symmetry of the Γ-*X* and Γ-*M* axes, the corresponding non-collinearly coupled B-modes are two-fold degenerate and can hybridize into pseudo-TE and pseudo-TM modes [17], hence a strong TM component appeared with the B-mode coupling even though the primary EL light generated from the MQW is TE polarized. The TE and TM modes for the present B-modes are degenerate and can be checked by the overlapping of the B-type mode lines in TE and TM orientations in Fig. 4(a) and 4(b). These doubly degenerate bands are reduced to the symmetric and antisymmetric coupled states results in the E field running perpendicular and parallel to the propagation directions and forms the TE and TM polarization states [18]. For the Γ-*X* directions there are two bands resulted from coupling with the four $G_{\Gamma X}$ wavevectors. One of the $G_{\Gamma X}$ wavevector is collinear with the Γ-*X* direction and while the other is lying perpendicular to the Γ-*X* direction to provide non-collinear coupling with the modes propagating in the Γ-*X* direction. The non-collinear coupling forms the two degenerate states while the collinearly coupled band is signally degenerate. Since the Bragg diffraction preserves the polarization, the emitted light from the singly degenerate band will have strong *s*-polarization. The doubly degenerate bands however will then possess a mixed *s*- and *p*-polarization. This can be revealed more clearly by looking at the calculated field distribution of the bands that E-field distributions of Bloch modes were calculated by 2D plane-wave expansion (PWE) method such as the same in Ref. 18, as shown in Fig. 4(c) and 4(d). As can be seen that the distribution is for the collinearlly coupled bands shows strongly parallel field distribution while the non-collinearly coupled bands posses a mixed field distribution pattern, hence a mixed state of polarization.

To examine the azimuthal anisotropy of the far-field distribution, the angular-resolved spectra of the out-coupled modes were measured as a function of the azimuthal angles (θ) with the sample rotated around the axis perpendicular to the wafer surface with 1 degree resolution. These spectra were then displayed on a wavelength vs. angle plot with the color of the pixels representing the intensity of the spectra according to the color-coded scale bar shown in Fig. 5. The angular-resolved spectra of different azimuthal angles show the evolution of the extraction of the collinearly and non-collinearly coupled guided modes. The intensity data at a fixed wavelength were taken from each spectrum for each azimuthal angle and plotted on the polar plot as different color of the pixels according to the colored scale bar shown. The radial length corresponding the magnitude of the in-plane component $k_{//}$. This plot corresponds to the far-field distribution at a fixed wavelength around the vertical axis. Figure 7 is the plot for the present sample at the different frequency a/λ. Figure 7(d) shows the circle and cross labels correspond to the "A" and "B" modes, respectively. The arcs are the contours of the resultant wavevectors after coupling to the reciprocal lattice wavevectors [19]. Figure 6(a) illustrates the formation of the contours for coupling respectively to $G_{\Gamma X}$ reciprocal wavevectors. As the sample rotates around the

#107988 - $15.00 USD Received 2 Mar 2009; revised 4 May 2009; accepted 5 May 2009; published 11 May 2009

vertical axis from the Γ-*X* direction, the alignment of the propagation direction to the $G_{\Gamma X}$ wavevector is changing from collinear to non-collinear. The resultant wavevector is tracing out an arc with the radius of curvature equals to the waveguide circle inside the air cone.

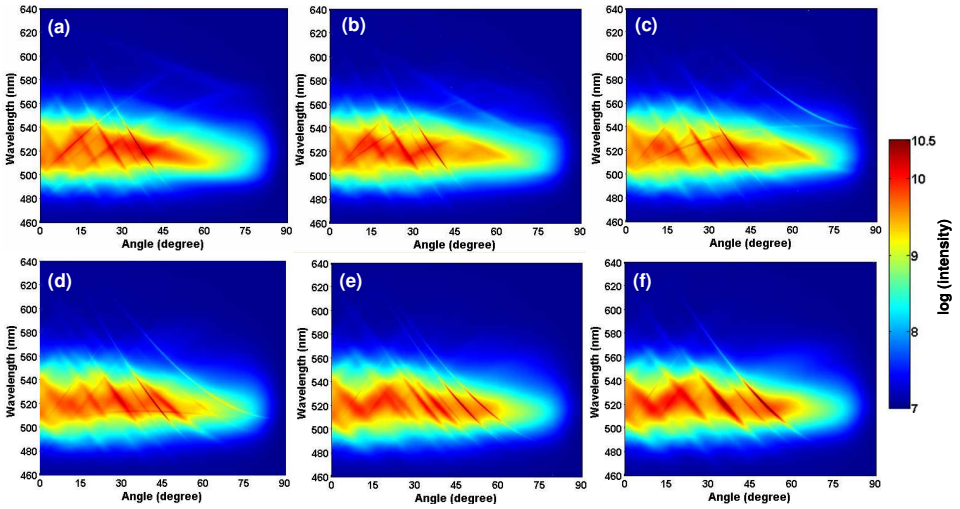

Fig. 5. (Media 1) Angular-resolved EL spectrum of the GaN PhC FT-LEDs measures along the (a) Γ-*X* direction ($\theta = 0$ degree), (b) $\theta = 10$ degree, (c) $\theta = 20$ degree, (d) $\theta = 30$ degree, (e) $\theta = 40$ degree and (f) Γ-*M* direction ($\theta = 45$ degree).

Different waveguide mode with different effective index will trace out an arc with the radius corresponding to the respective waveguide circle as shown in Fig. 6(a). The five arcs correspond to the five modes that shown in Fig. 7(d). Similarly, the coupling with the $G_{\Gamma M}$ wavevector is shown in Fig. 6(b) with the two modes corresponding to that appear in Fig. 7(d). As explained above, the coupling to $G_{\Gamma M}$ is weaker since it is longer than $G_{\Gamma X}$. Thus, it can be seen that the collinearly coupled A-type modes for the Γ-*X* direction turn into the non-collinearly B-type modes in the Γ-*M* directions as the sample is rotated by $\pi/4$ and vise versa for the modes in the Γ-*M* directions. Since the A-type modes are TE polarized and B-type modes are TE and TM polarized [6], it is expected that polarization along the arcs will be varying from that of the A-type to that of the B-type modes. This complicated polarization distribution of the extracted light will have implication when PhC LED is used as the light source, since they depends on the reflective properties light. Knowledge of the polarization distribution due to PhC is therefore indispensable.

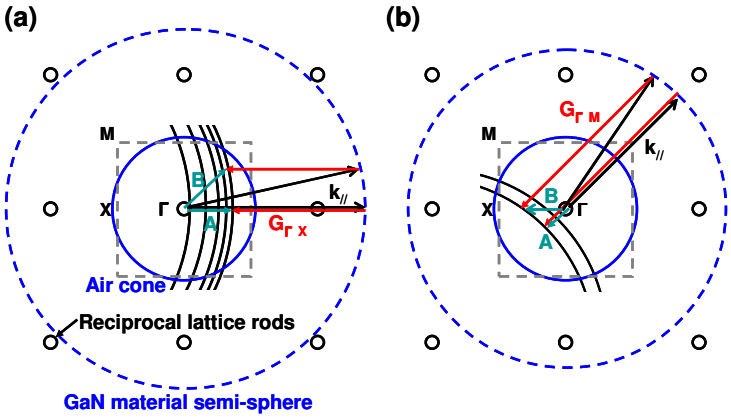

Fig. 6. Azimuthal scan of the light extracted distribution. Part (a) and (b) illustrate the formation of the contours corresponding to the coupling of different n_{eff} of the multimodes to the reciprocal wavevectors (a) $G_{\Gamma X}$ and (b) $G_{\Gamma M}$. The blue dash and blue solid circles

#107988 - $15.00 USD Received 2 Mar 2009; revised 4 May 2009; accepted 5 May 2009; published 11 May 2009

indicate the waveguide circle with radius $n_{eff}k_o$ and the light cone, respectively. The gray square is the reduced Brillouin zone boundary.

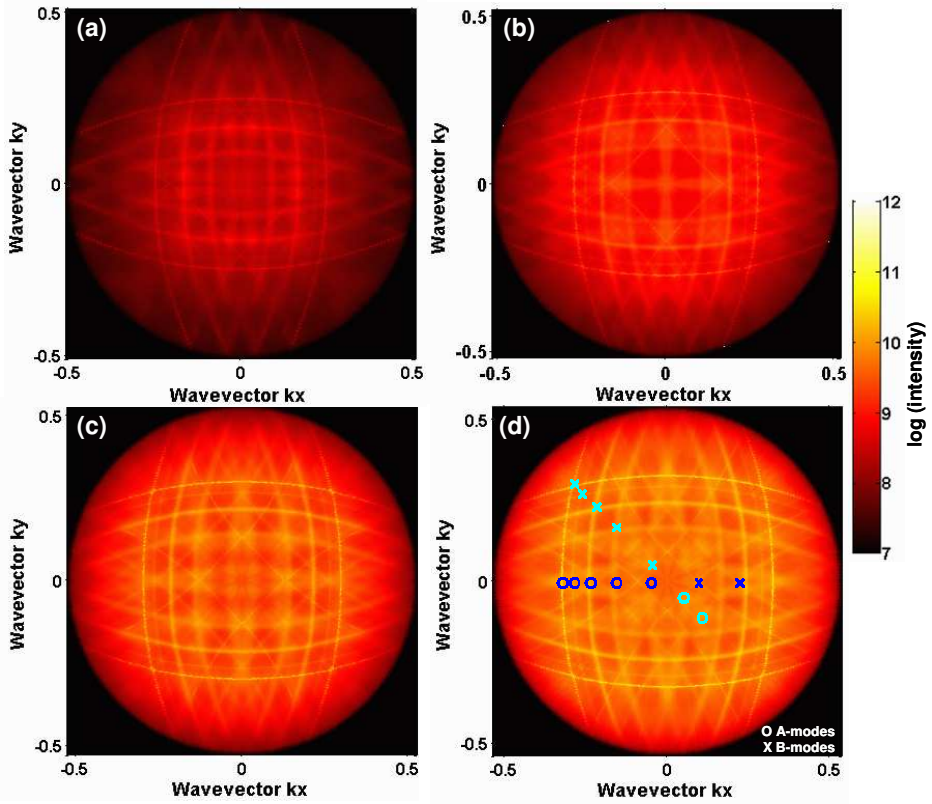

Fig. 7. (Media 2) The maps are the intensity of the extracted light at the different wavelength around the azimuthal direction with 1 degree resolution. The data are taken from 0 to 45 degree then unfolded to fill the full circle. The wavelength was kept at a constant corresponding to (a) a/λ = 0.509, (b) a/λ = 0.518, (c) a/λ = 0.528, and (d) a/λ = 0.538, respectively. The radius of the plot is the magnitude of the in-plane component.

The wavelength-integrated far-field pattern from the GaN PhC FT-LED is shown in Fig. 8(a) which reveals the PhC diffraction patterns with four-fold symmetry due to square lattice. The detailed radiation patterns also show a stronger enhancement around the vertical direction. The angular distribution radiation patterns of the light output from the GaN PhC FT-LEDs and the GaN FT-LEDs without PhC have been measured at a driving current of 350 mA, as shown in Fig. 8(b). At 50% intensity of each device, it can be seen that the GaN PhC FT-LEDs show higher extraction efficiency with a collimation angle 102.3° and 116.4° in the Γ-*X* and Γ-*M* direction of respectively. The measured far-field pattern of the GaN FT-LED without PhC is nearly Lambertian. Furthermore the far-field emission pattern, normalized with the peak intensity, remains unchanged when current is varied from 20 to 500 mA. This invariance of the far-field pattern indicates the temperature stability of the device since the junction temperature of the device can vary significantly over this current range (>100°C). Such stability is expected from the material properties of the GaN systems and the PhC structure.

#107988 - $15.00 USD Received 2 Mar 2009; revised 4 May 2009; accepted 5 May 2009; published 11 May 2009

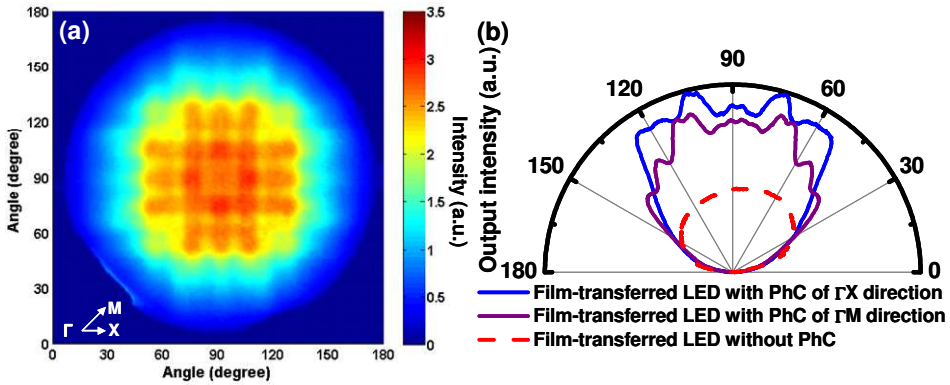

Fig. 8. (a) Top-view 3D far-field pattern of the GaN PhC FT-LED with the square lattice. (b) Angular distribution radiation pattern of the GaN PhC FT-LED with Γ-*X* and Γ-*M* direction.

4. Conclusions

In conclusion, angular-resolved EL measurement revealed strong guided modes extraction based on the Bragg's diffraction via PhC effect in the GaN PhC FT-LEDs. Both A and B-type modes are identified and their dispersions are found to be in agreement for the free photon band structure indicating the shallow holes etching in the present sample. In addition, the azimuthal-mapping at fixed wavelength shows the evolution of the collinear and non-collinear modes. The pseudo-TM behavior for the non-collinearly coupled modes was observed. Furthermore, the light enhancement of ~2.7x and the collimation angle about 102.3° from GaN PhC FT-LED were achieved. The present results indicate that the PhC enhanced FT-LED will have complicated polarization distribution which will have implication for the use of these LEDs as the light sources.

Acknowledgements

The authors gratefully acknowledge Dr. S. C. Wang and Dr. T. C. Lu at National Chiao-Tung University (NCTU) in Taiwan for their technical support.

#107988 - $15.00 USD Received 2 Mar 2009; revised 4 May 2009; accepted 5 May 2009; published 11 May 2009